Electronic Supplementary Information (ESI)

Co-doping regulation on Ni-based electrocatalyst to adjust the selectivity of oxygen reduction reaction for Zn-air battery and H2O2 production

Songhan Hu[a, b], Kai Wang [a]*, Xinxin Xu[c], Qiang Wang[a]*

[a] Key Laboratory of Electromagnetic Processing of Materials (Ministry of Education), Northeastern University, Shenyang 110819, China

[b] School of Materials Science and Engineering, Northeastern University, Shenyang 110819, China

[c] Department of Chemistry, College of Science, Northeastern University, Shenyang 110819, Liaoning, China

Materials and characterization

All chemicals were of analytical grade, commercially available from Sinopharm Chemical Reagent Co. Ltd and used as received without further purification. XRD pattern was recorded on X-ray diffractometer with CuKα (λ = 1.5418 Å) radiation (Philips X'Pert Pro Super, Philips).Raman spectroscopy was conducted with an excitation wavelength of 633 nm (LabRAMHR-800, HORIBA). XPS was performed on photoelectron spectroscopy (ESCALAB 250Xi, Thermo Fisher Scientific). The morphology was observed on an ultra plus field emission scanning electron microscope (SEM, ultra plus, ZEISS) and Spherical aberration corrected transmission electron microscope (ACTEM, JEOL, EM-ARM200F). Electrochemical experiments were conducted on electrochemical workstation (CHI-760E, Chenhua). UV-Vis spectrophotometer (T6 new century, Persee) was used to study the concentration of H_2O_2.

Single-crystal X-ray diffraction

Single crystal of **NiMOF** was selected under an optical microscope and glued on a glass fiber. Structural measurement was performed with a Bruker AXS SMART APEX II CCD diffractometer at 293 K. The structure was solved with direct method and refined by the full-matrix least-squares method on F^2 with the Olex2 crystallographic software package. Anisotropic thermal parameters were used to refine all non-hydrogen atoms. Carbon-bound hydrogen atoms were placed in geometrically calculated positions.CIF file (CCDC 2350292) contains supplementary crystallographic data for this paper. The file can be obtained free of charge via www.ccdc.cam.ac.uk/data_request/cif (Cambridge Crystallographic Data Centre).

The synthesis of NCNT

Zinc nitrate (0.6 g) and 2-methylimidazole (1.3 g) were dissolved in methanol (10.0 ml) with the separated glass jar. Then, the zinc nitrate solution was rapidly poured into the 2-methylimidazole solution under constant stirring at 25 °C. The mixed solution was stirred for 15 min and kept the solution at tranquility condition for 24 h. The final products were collected by centrifuging rinsed with excess methanol, and dried in an oven at 80 °C for 12 h. Then ZIF-8 was obtained. ZIF-8 (0.2 g, at gas outlet side) and DCDA (2.2 g, at gas inlet side) were placed on both sides of a porcelain boat. After heating in the presence of N_2 atmosphere in tube furnace at 800 °C for 3 h, NCNT was obtained.

The synthesis of Co/NCNTs

The ZIF-67 was synthesized by mixing cobalt chloride (0.125g) and 2-methylimidazole (0.33g) in 10 ml methanol under stirring for 12 h. After filtering precipitates and washing products with methanol for many times, the products were dried at 80 °C overnight to obtain ZIF-67 powder. ZIF-67 (0.2 g, at gas outlet side) and DCDA (2.2 g, at gas inlet side) were placed on both sides of a porcelain boat. After heating in the presence of N_2 atmosphere in tube furnace at 800 °C for 3 h, Co/NCNTs was obtained.

RRDE test in ORR

RRDE (electrode area is 0.2475 cm^2) experiment was also conducted in O_2 saturated KOH (0.1 M). Working electrode was fabricated as follows: the mixture of **NiO@NCNTs**(or **Co/NiO@NCNTs**, 10 mg) was dispersed in aqueous solution of N,N-Dimethylformamide (0.9 mL) and Nafion (100 µL, 5 %). The ink (3 µL) was dropped on RRDE and served as working electrode. Pt wire and Ag/AgCl electrode (3 M KCl) were employed as counter and reference electrodes. The disk potential was cycled from 0 to 1.0 V (vs. RHE) with a scan rate of 10 $mV \cdot s^{-1}$. The ring potential was constant at 1.2 V (vs. RHE). The H_2O_2 selectivity and electron transfer number (n) were calculated with Eq. 1 and 2. In these equations, ID and IR represent the disk and ring currents density. N (N = 0.37, obtained from $K_3Fe(CN)_6$ reduction experiments at various rotation rates) is

the current collection efficiency of the Pt ring[1].

$$H_2O_2\ \% = (200 \times IR/N)/ (IR/N + ID)\ (1)$$

$$n = 4 \times Id/(IR/N + ID)\ (2)$$

RDE test in ORR

The ink was obtained as above mentioned and cast on rotating disk electrode (RDE). The RDE served as working electrode. Carbon rod and Ag/AgCl electrode were used as counter and reference electrodes. ORR was performed in 0.1 M KOH. In ORR, linear sweep voltammetry (LSV) curves were recorded at 10 $mV \cdot s^{-1}$. The rotating speed of RDE was 400, 625, 900, 1225 and 1600 rpm. The electron transfer number (n) can also be calculated by the Koutecky-Levich (K-L) method (3-5)[2]:

$$1/J_{disk} = 1/J_k+1/J_l (3)$$

$$J_l=0.62\times n\times F\times D^{2/3}\times v^{-1/6}\times C^*\times \omega^{1/2}\ (4)$$

$$1/J_{disk}= 1/J_k+ 1/0.62\times n\times F\times D^{2/3}\times v^{-1/6}\times C^*\times \omega^{1/2}\ (5)$$

where J_{disk} represents disk current density, J_k and J_l are the kinetic and diffusion limiting current density, respectively, F is the faraday constant, D is the diffusion coefficient of O_2, v is the kinematic viscosity of electrolyte, C* is the concentration of O_2 in the bulk electrolyte, and ω is the angular velocity (rad/s) of disk electrode.Therefore, n can be derived from the slope of the linear graph of $1/J_{disk}$ and $\omega^{-1/2}$.

H_2O_2 concentration measurement and stability test

The H_2O_2 production was carried out in a homemade two-room cell electrolyzer with a three-electrode configuration. First, 200 μL of the as-prepared ink was uniformly deposited on the carbon paper of 1 cm ×1 cm and dried in the air. Then the carbon cloth with a mass load of 0.1 mg was used as the working electrode, the carbon rod as the counter electrode, and Ag/AgCl as the reference electrode, to perform the electrosynthesis of H_2O_2 in a self-made H-type electrolytic cell. A Nafion 117 membrane was adopted to separate the cathode and anode chambers. The production rate of H_2O_2 was quantified by the titration of cerium sulfatewith Eq. 6[3].

$$2Ce^{4+}+H_2O_2 \rightarrow 2Ce^{3+}+2H^++O_2 (6)$$

Zn-air battery assemble

The hybrid battery was assembled with a home-made cell in the size 4.2 × 4 × 4 cm^3. In this battery, the Zn plate acts as anode with working area 3.2 cm^2. The ink of Co/NiO@NCNTswas cast on carbon paper at first. Its other side was covered by PTFE and used as air diffusion layer. After covered by PTFE, the carbon paper with Co/NiO@NCNTs loaded on was employed as cathode. The working area of air cathode is also 3.2 cm^2. In this hybrid battery, mixture solution of KOH (6.0 M) and $Zn(OAc)_2 \cdot 2H_2O$ (20 mM) was used as electrolyte. In measurement, no additional oxygen was inlet into this battery. The specific capacitance of battery was calculated based on Eq. 7. In this equation, I and t are current density and discharge time. Δm_{Zn} represents the mass of Zn consumed[4].

$$C= It/\Delta\ m_{Zn}\ (7)$$

Calculation methods

All the computational analysis was performed employing the Gaussian 09 program package. The unrestricted hybrid density functional method UB3LYP was used in the density function theory (DFT) calculation. The adsorption energy was calculated using Eq. 8[5].

$$\Delta G = \Delta E + ZPE - TdS\ (8)$$

Table. S1 Crystallographic data for NiMOF.

Complex	NiMOF
Empirical formula	$C_9H_{11}N_2NiO_{7.50}$
Formula weight	325.91
Crystal system	Monoclinic
Space group	*I*2/*a*
***a* (Å)**	19.1436(9)
***b* (Å)**	9.0562(3)
***c* (Å)**	12.8706(5)
***α* (°)**	90
***β* (°)**	93.528 (4)
***γ* (°)**	90
***V* (Å^3)**	2227.12(15)
Z	8
***D$_c$*(g cm^{-3})**	1.944
***μ* (mm^{-1})**	1.783
***F* (000)**	1336
Reflections collected	5561
Unique reflections	2603
parameters	185
R_{int}	0.064
GOF	1.085
R_1^a [I>2σ(I)]	0.0240
wR_2^b (all data)	0.0582
$^aR_1 = \Sigma\|\|F_o\|-\|F_c\|\|/\Sigma\|F_o\|$, $^bwR_2 = \Sigma[w(F_o^2-F_c^2)^2]/\Sigma[w(F_o^2)^2]^{1/2}$	

Table. S2 Selected bond distances (Å) and angles (°) for **NiMOF**.

NiMOF			
Ni(1)-O(16)#1	2.1005(12)	Ni(1)-O(17)	2.0934(12)
Ni(1)-O(13)	2.0298(11)	Ni(1)-O(18)	2.0497(11)
Ni(1)-O(15)#1	2.1503(12)	Ni(1)-N(5)#2	2.0477(14)
Ni(1)-C(14)#1	2.4595(16)	O(16)#1-Ni(1)-O(15)#1	61.96(4)
O(16)#1-Ni(1)-C(14)#1	31.09(5)	O(13)-Ni(1)-O(16)#1	160.90(5)
O(13)-Ni(1)-O(15)#1	98.98(5)	O(13)-Ni(1)-O(17)	92.08(5)
O(13)-Ni(1)-O(18)	90.49(5)	O(13)-Ni(1)-N(5)#2	99.20(5)
O(13)-Ni(1)-C(14)#1	129.82(5)	O(15)#1-Ni(1)-C(14)#1	30.86(5)
O(17)-Ni(1)-O(16)#1	86.40(5)	O(17)-Ni(1)-O(15)#1	87.88(4)
O(17)-Ni(1)-C(14)#1	86.28(5)	O(18)-Ni(1)-O(16)#1	89.11(5)
O(18)-Ni(1)-O(15)#1	85.50(5)	O(18)-Ni(1)-O(17)	173.20(5)
O(18)-Ni(1)-C(14)#1	87.24(5)	N(5)#2-Ni(1)-O(16)#1	99.88(5)
N(5)#2-Ni(1)-O(15)#1	161.81(5)	N(5)#2-Ni(1)-O(17)	92.00(5)
N(5)#2-Ni(1)-O(18)	93.80(5)	N(5)#2-Ni(1)-C(14)#1	130.97(6)
Symmetry code for**NiMOF**:#1 -x+1,y+1/2,-z+3/2 #2 -x+1/2,-y+3/2,-z+3/2			

Table S3. Compare H_2O_2 production ability of **NiO@NCNTs** with other 2e-ORR electrocatalysts.

Electrocatalysts	Electrolyte	H_2O_2 Selectivity (%@V vs. RHE)	Production rate	Refs
NiO@NCNTs	0.1 M KOH	90.5~ 95.2%@0.46	500 mmol g^{-1} h^{-1}	This work
ZnO	0.1 M KOH	90.4@0.4	211.94 mmol g^{-1} h^{-1}	[6]
NiO	0.1 M KOH	79.4@0.4	167.47 mmol g^{-1} h^{-1}	[6]
h-WO_3	0.1 M KOH	71@0.4	128 mmol g^{-1} h^{-1}	[7]
γ-WO_3	0.1 M KOH	78@0.4	145 mmol g^{-1} h^{-1}	[7]
oxo-G/H_2O2/ $NH_3{\cdot}H_2O$	0.1 M KOH	82@0.4	224.8 mmol g^{-1} h^{-1}	[8]
Mo-TiO_2	0.1 M KOH	86@0.68	395.3 mmol g_{cat}^{-1} h^{-1}	[9]
HNCS	0.1 M KOH	~91.9	618.5mmol g_{cat}^{-1} h^{-1}	[10]
g-N-CNHs	0.1 M KOH	0.71	73 mmol g^{-1} h^{-1} cm^{-2}	[11]

Table S4. Compare the ORR activity of **Co/NiO@NCNTs** with other electrocatalysts.

Catalysts	Electron transfer number	Half-wave potential ($E_{1/2}$, V)	Current density ($mA \cdot cm^{-2}$)	Tafel slope (mV· dec-1)	Refs
Co/NiO@NCNTs	3.8	0.83	6.21	43	This work
FexN-NC	≈4	0.873	5.7	90	[12]
Co-NCNTs/CNF	≈3	0.79	NA	67.33	[13]
Co_{SA}Ni-NCNT/CNF	≈4	0.86	NA	58	[13]
Co@Co_3O_4/NCNT	3.8	0.76	NA	83	[14]
NiFeVS	3.8	0.759	NA	82.5	[15]
30-ZnMn-NC	3.8	0.83	NA	80.9	[16]
ZIF-Co_3O_4/NCF	3.7	0.813	NA	72	[17]

NA = not attained.

Table S5. Compare the performance of Zn-air battery based on **Co/NiO@NCNTs** with others.

Catalysts	Power density ($mW\ cm^{-2}$)	Specific capacity ($(mA\ h\ g^{-1})$)	Current density ($mA{\cdot}cm^{-2}$)	Refs
Co/NiO@NCNTs	73.8	779.3	5	This work
Co_{SA}Ni-NCNT/CNF	70.39	803.5	10	[13]
MCO/CNFs@NC	75	742	5	[18]
NiO/CoN PINWs	79.6	490	5	[19]
Ni-N4/GHSs/Fe-N4	NA	777.6	5	[20]
NiCo/NCNTs	65	NA	NA	[21]

NA = not attained.

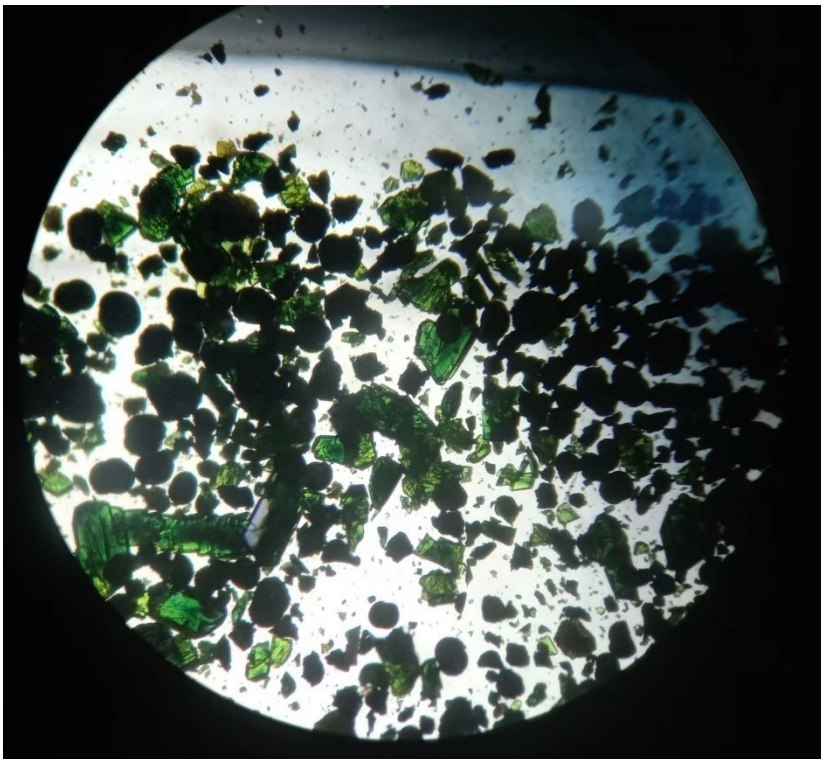

Fig. S1. Morphology of crystalline **NiMOF** under optical microscope.

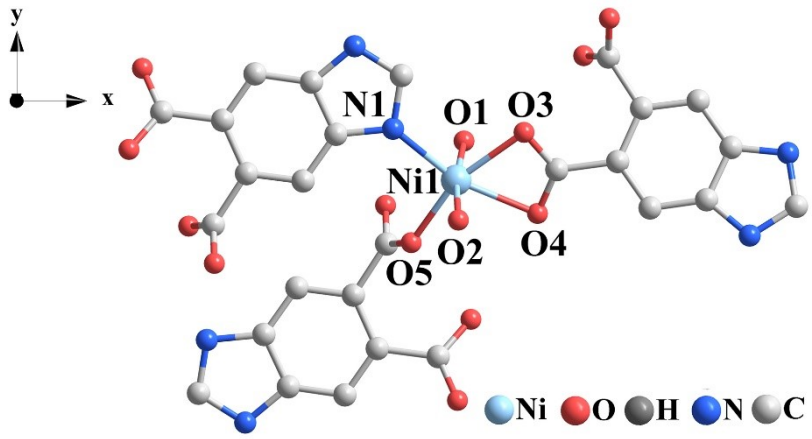

Fig. S2. The coordination environment of the Ni^{2+}.

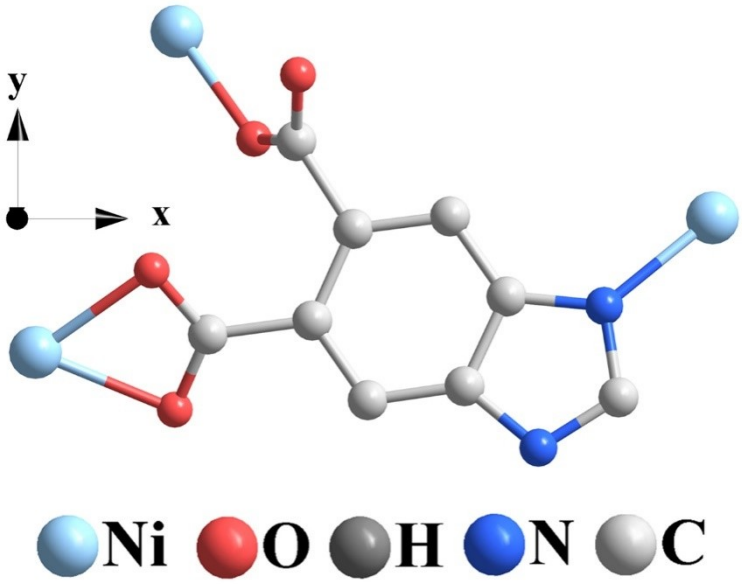

Fig. S3. The coordination environment of the BZIDA

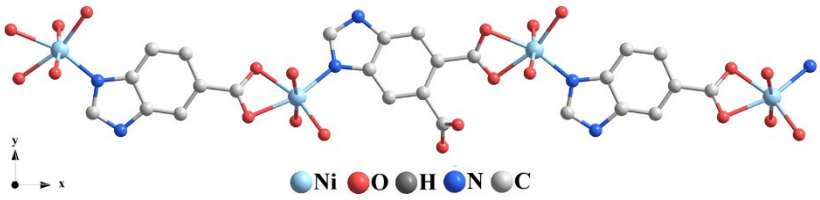

Fig. S4. One-dimensional chain-like structure of **NiMOF**.

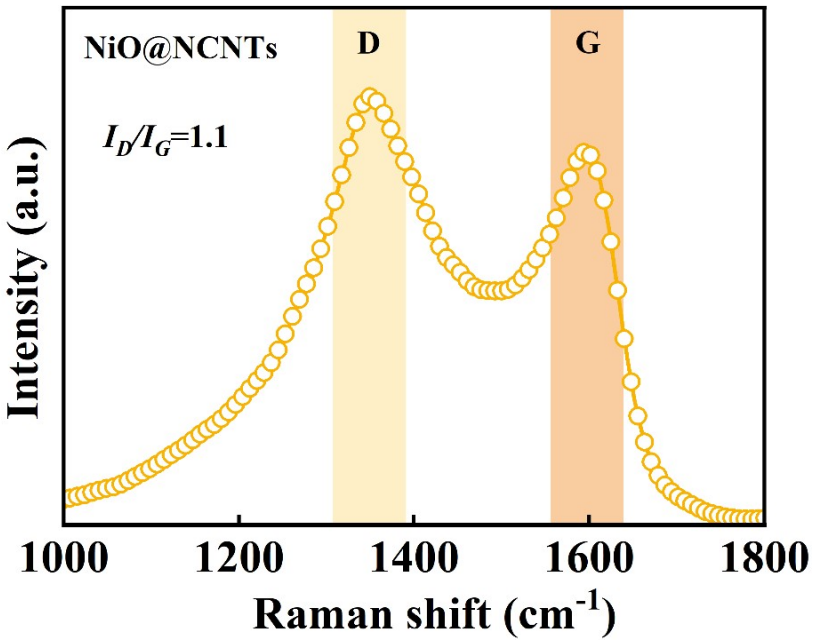

Fig. S5. Raman spectrum of **NiO@NCNTs**.

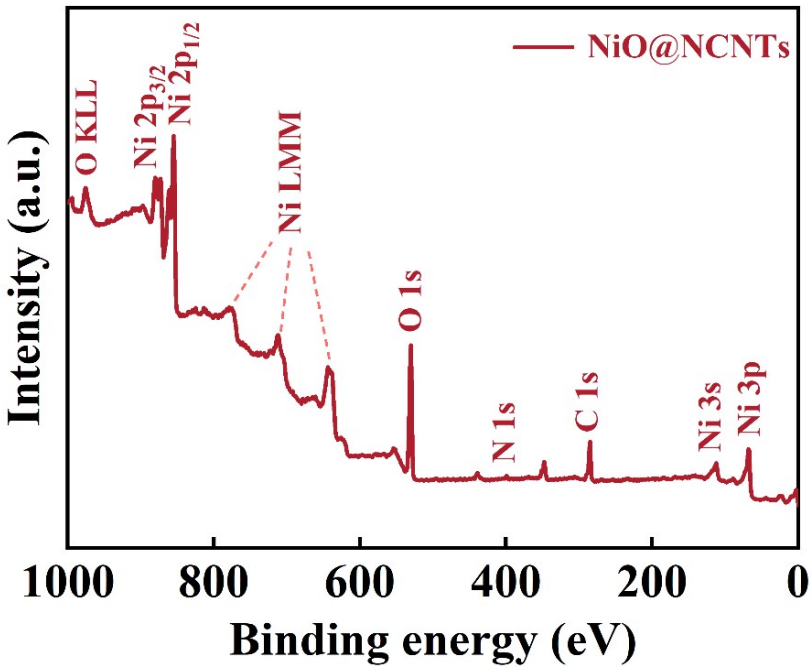

Fig. S6. XPS survey spectrum of**NiO@NCNTs**.

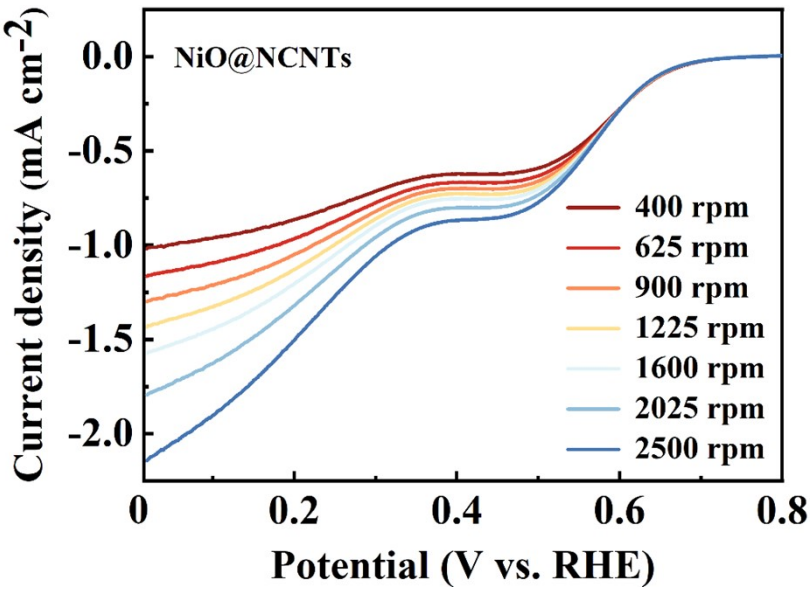

Fig. S7. LSV curves of **NiO@NCNTs** at different rotation speeds.

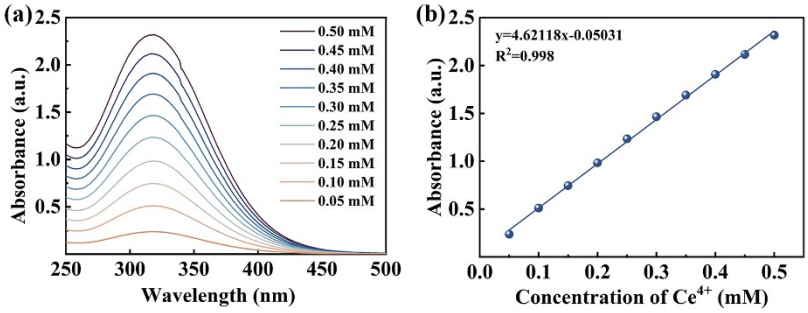

Fig. S8. (a) Absorbance spectra of standard $Ce(SO4)_2$ solutions in 0.5 M H_2SO_4; (b)the calibration curve of H_2O_2 concentration.

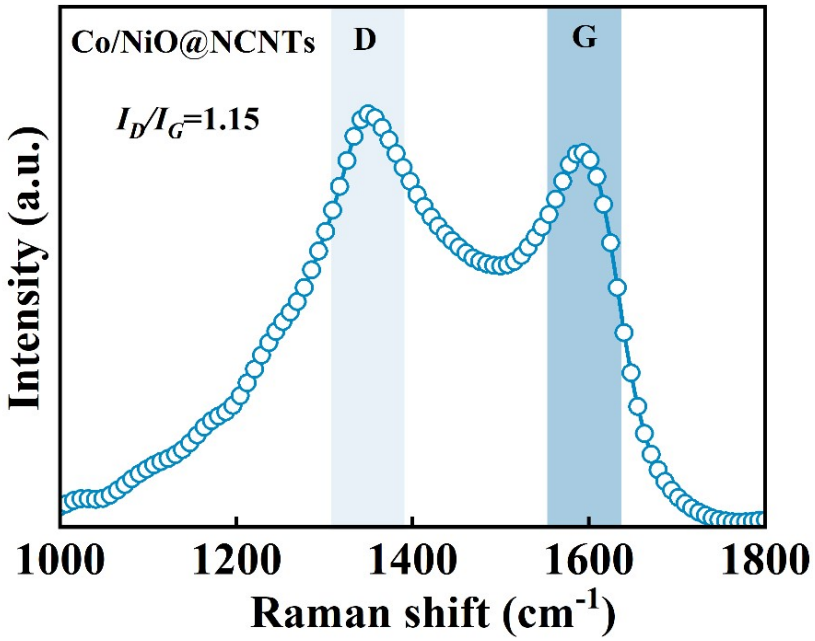

Fig. S9. Raman spectrum of **Co/NiO@NCNTs**.

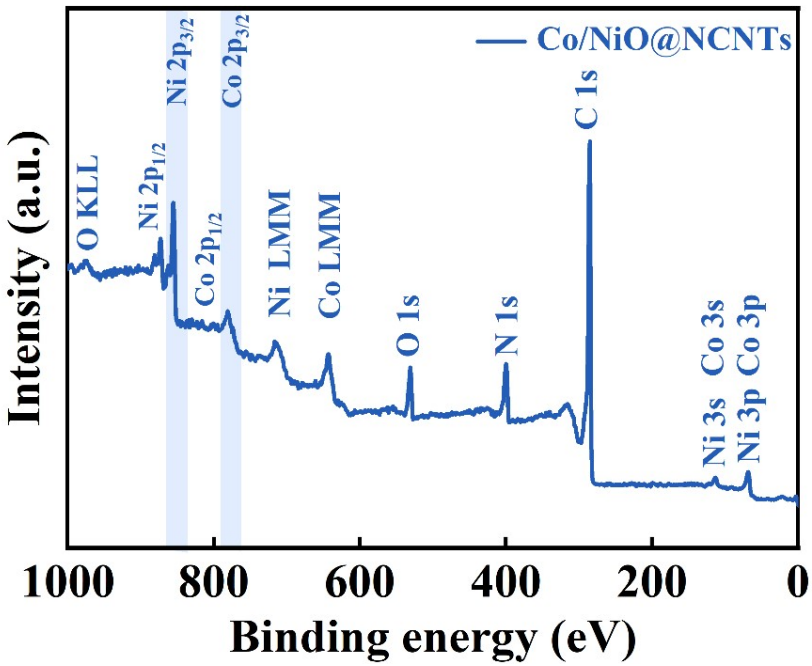

Fig. S10. XPS survey spectrum of **Co/NiO@NCNTs**.

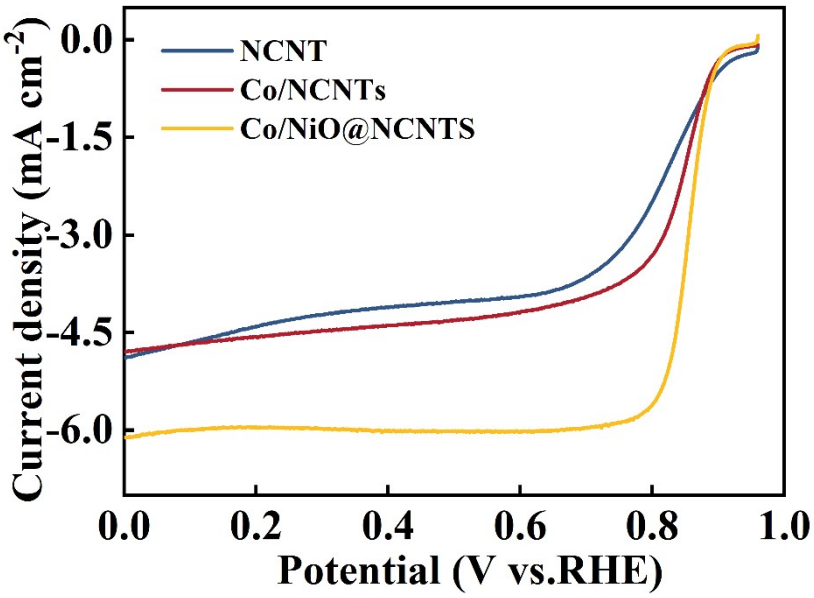

Fig. S11. LSV curves of NCNT, Co/NCNTs and Co/NiO@NCNTs at 1600 rpm.

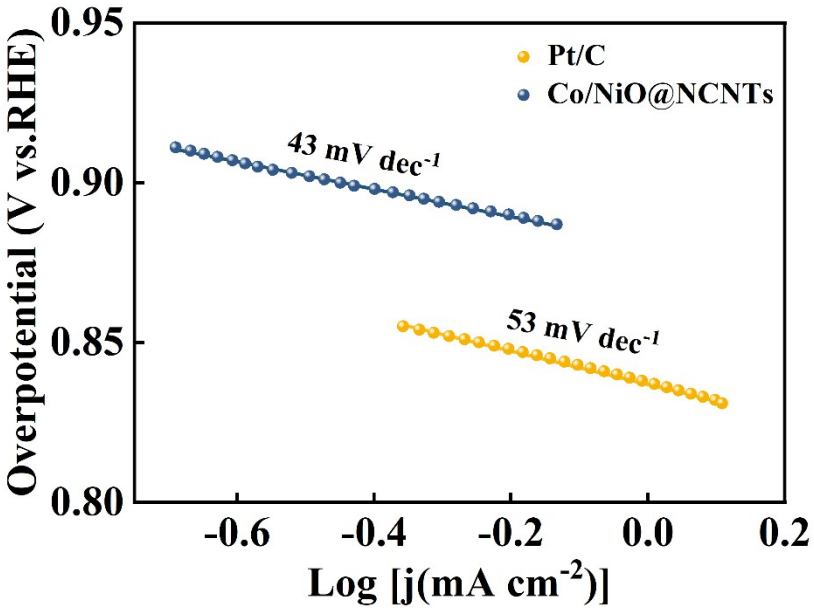

Fig. S12. Tafel plots of **Co/NiO@NCNTs** and Pt/C.

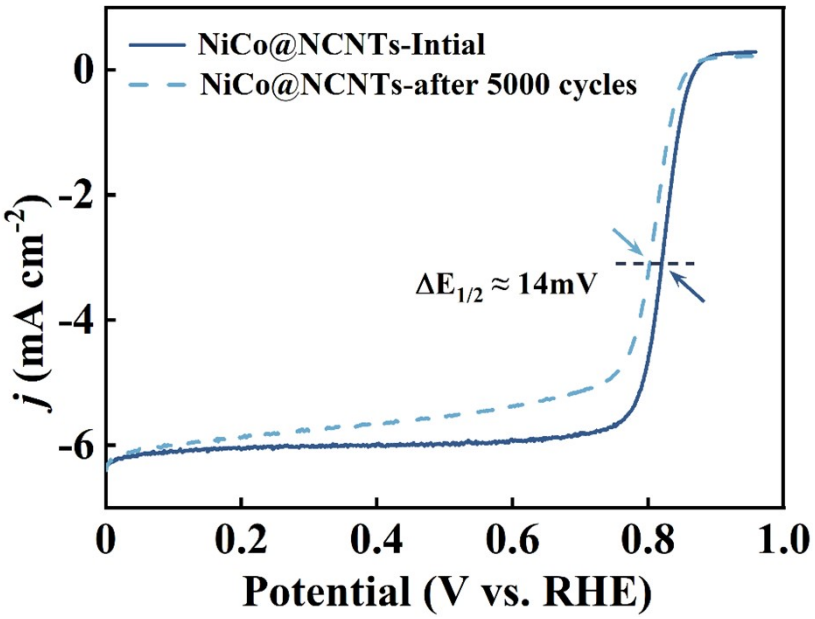

Fig. S13. ORR LSV curves in O_2 saturated 0.1 M KOH at 1600 rpm for the **Co/NiO@NCNTs** before and after 5000 CV cycles tests.

Reference

1. B. You, N. Jiang, M. Sheng, W.S. Drisdell, J. Yano, Y. Sun, *ACS Catal.*, 2015, **5**, 7068-7076.

2. A.K. U, A. Sethi, R.M. Lawrence, V.M. Dhavale, *Int. J. Hydrogen Energy*, 2021, **46**, 34701-34712.

3. M. Wang, N. Zhang, Y. Feng, Z. Hu, Q. Shao, X. Huang, *Angew. Chem., Int. Ed.*,2020, **59**, 14373-14377.

4. D. Xu, S. Wu, X. Xu, Q. Wang, *ACS Sustainable Chem. Eng.*, 2020, **8**, 4384-4391.

5. X. Ge, A. Sumboja, D. Wuu, T. An, B. Li, F.W.T. Goh, T.S.A. Hor, Y. Zong, Z. Liu, *ACS Catal.* 2015, **5** , 4643-4667.

6. Y. Zhang, H. Jiang, C. Zhang, Y. Feng, H. Feng, S. Zhu, J. Hu, *J. Mater. Chem. A*, 2024, **12**, 6123-6133.

7. H. Jiang, Y. Wang, J. Hu, X. Shai, C. Zhang, T. Le, L. Zhang, M. Shao, *Chem. Eng. J.*, 2023, **452**, 139449.

8. L. Han, Y. Sun, S. Li, C. Cheng, C.E. Halbig, P. Feicht, J.L. Hübner, P. Strasser, S. Eigler, *ACS Catal.*, 2019, **9**, 1283-1288.

9. Z. Deng, C. Ma, S. Yan, J. Liang, K. Dong, T. Li, Y. Wang, L. Yue, Y. Luo, Q. Liu, Y. Liu, S. Gao, J. Du, X. Sun, *Catal. Sci. Technol.*, 2021, **11**, 6970-6974.

10. Y. Hu, J. Zhang, T. Shen, Z. Li, K. Chen, Y. Lu, J. Zhang, D. Wang, *ACS Appl. Mater. Interfaces*, 2021, **3**, 29551-29557.

11. D. Iglesias, A. Giuliani, M. Melchionna, S. Marchesan, A. Criado, L. Nasi, M. Bevilacqua, C. Tavagnacco, F. Vizza, M. Prato, P. Fornasiero, *Chem.*, 2018, **4**, 106-123.

12. S. Wu, X. Liu, H. Mao, J. Zhu, G. Zhou, J. Chi, Z. Wu and L. Wang, *Adv. Energy Mater.,* 2024, **14**, 2400183.

13. M. B. Poudel, M. P. Balanay, P. C. Lohani, K. Sekar and D. J. Yoo, *Adv. Energy Mater.,* 2024,2400347.

14. J. Xiao, C. Chen, J. Xi, Y. Xu, F. Xiao, S. Wang and S. Yang, *Nanoscale,* 2015, **7**,7056-7064.

15. F. N. I. Sari, Y.-C. Lai, Y.-J. Huang, X.-Y. Wei, H. Pourzolfaghar, Y.-H. Chang, M. Ghufron, Y.-Y. Li, Y.-H. Su, O. Clemens and J.-M. Ting, *Adv. Funct. Mater.,* 2024, **34**,2310181**.**

16. L. Wang, M. Xu, H. Li, Z. Huang, L. Wang, T. Taylor Isimjan and X. Yang, *Inorg. Chem,* 2023, **62**,13284-13292.

17. L. Song, J. Tang, T. Wang, C. Wu, Y. Ide, J. He and Y. Yamauchi, *Chem. Eur. J.,* 2019, **25**,6807-6813.

18. T. T. Gebremariam, F. Chen, Q. Wang, J. Wang, Y. Liu, X. Wang and A. Qaseem, *ACS Appl. Energy Mater.,* 2018, **1**,1612-1625.

19. J. Yin, Y. Li, F. Lv, Q. Fan, Y.-Q. Zhao, Q. Zhang, W. Wang, F. Cheng, P. Xi and S. Guo, *ACS Nano,* 2017, **11**,2275-2283.

20. J. Chen, H. Li, C. Fan, Q. Meng, Y. Tang, X. Qiu, G. Fu and T. Ma, *Adv. Mater.,* 2020, **32**,003134.

21. S. Hanif, N. Iqbal, X. Shi, T. Noor, G. Ali and A. M. Kannan, *Renewable Energy,* 2020, **154**,508-516.